horticulturae

MDPI

Article

Responses of *Paspalum vaginatum* Root to Salt Stress: Integrating Morphological, Physiological, and Root Electrochemical Traits

Shengnan Yang [1,†], Dongli Hao [2,†], Zhiyong Wang [1], Junqin Zong [2], Li Liao [1], Hailong Lu [2], Xi Xiang [2], Zhengyang Liu [3] and Ling Li [2,*]

[1] College of Tropical Agriculture and Forestry, Sanya Institute of Breeding and Multiplication, Hainan University, Haikou 571737, China; 23210834000011@hainanu.edu.cn (S.Y.); wangzhiyong@hainanu.edu.cn (Z.W.); liaoli@hainanu.edu.cn (L.L.)
[2] Jiangsu Key Laboratory for Conservation and Utilization of Plant Resources, Institute of Botany, Jiangsu Province and Chinese Academy of Sciences (Nanjing Botanical Garden Mem. Sun Yat-Sen), Nanjing 210014, China; haodongli@jib.ac.cn (D.H.); luhailong@jib.ac.cn (H.L.); xiangxi202601@163.com (X.X.)
[3] College of Forestry and Landscape Architecture, South China Agricultural University, Guangzhou 510642, China; liuzy2002@stu.scau.edu.cn
* Correspondence: liling@jib.ac.cn
† These authors contributed equally to this work.

Abstract

Elucidating the response mechanisms of seashore paspalum (*Paspalum vaginatum*) roots to salt stress is crucial for breeding salt-tolerant varieties. This study aimed to investigate the morphological, physiological, and surface electrochemical responses of seashore paspalum roots to salt stress. The salt-tolerant genotype Sealsle2000 and salt-sensitive genotype 17U-45 were subjected to 300 mM salt stress for 4 and 8 days. Results showed that salt stress exerted a more pronounced inhibitory effect on root growth than on shoot growth, with Sealsle2000 exhibiting less growth inhibition compared to 17U-45. Under salt stress, Sealsle2000 adsorbed more Na^+ on the root surface and sequestered them within the roots than 17U-45; furthermore, Sealsle2000 was able to maintain higher K^+/Na^+ ratios. In terms of physiological mechanisms, Sealsle2000 maintained higher activities of superoxide dismutase and catalase, as well as elevated levels of osmotic adjustment substances (proline and soluble sugars) in roots, which collectively alleviated membrane lipid peroxidation damage and osmotic stress. Compared to 17U-45, Sealsle2000 possessed more negative charges and functional groups on the root surface, which contributed to its higher Na^+ adsorption capacity and enhanced salt tolerance. Collectively, these findings establish a theoretical framework for understanding the salt tolerance mechanisms of seashore paspalum and other plants.

Keywords: salinity; *Paspalum vaginatum*; root; sodium absorption; root surface charge

Check for updates

Received: 23 January 2026
Revised: 19 February 2026
Accepted: 27 February 2026
Published: 28 February 2026

Copyright: © 2026 by the authors. Licensee MDPI, Basel, Switzerland. This article is an open access article distributed under the terms and conditions of the Creative Commons Attribution (CC BY) license.

1. Introduction

Soil salinization is one of the major abiotic stresses affecting the sustainable productivity of global crops. According to statistics from the Food and Agriculture Organization of the United Nations (FAO), the global area of saline–alkali land amounts to 1381 million hectares, accounting for nearly 10.7% of the total terrestrial area, and this area is expanding at an annual rate of 1–1.5 million hectares [1]. In China, saline–alkali land covers 36 million hm^2, representing 4.88% of the country's available land [2]. The accumulation

of toxic ions (mainly Na^+ and Cl^-) of saline–alkali lands impairs root water absorption, induces osmotic stress, and disrupts plant physiological and metabolic processes (e.g., reduced photosynthetic efficiency and imbalanced nutrient metabolism), ultimately leading to growth inhibition or even plant death [3–7]. As the primary plant organ in contact with soil, roots are the first to perceive salt stress signals. They then transmit these signals to shoot tissues via signal transduction, thereby initiating stress responses [8]. To adapt to salt stress, plants actively remodel their root system architecture by regulating root length, lateral root number, and growth direction, which optimizes water and nutrient uptake efficiency [9–11]. Notably, the effect of salt on root growth exhibits a distinct concentration dependence: Low-concentration salt generally promotes root growth (especially lateral root proliferation), while high-concentration salt reduced root lengths, lateral root number, and lateral root density [8,12]. Among these effects, salt-tolerant plants can usually expand their root absorption range by maintaining primary root elongation and increasing lateral root branching, thereby acquiring sufficient water and nutrients to adapt to salt stress [8]. Under salt stress, plant root systems maintain intracellular Na^+/K^+ homeostasis primarily through the mechanisms of selective ion absorption, ion extrusion, and vacuolar compartmentalization, thereby preventing the toxic effects of high Na^+ levels on plant cells and physiological metabolism [13,14]. Salt stress also induces excessive accumulation of reactive oxygen species (ROS) in plants, which causes oxidative damage such as membrane lipid peroxidation, protein denaturation, and nucleic acid degradation [15,16]. To mitigate such stress, roots rapidly activate dual protective mechanisms: enhancing the activities of antioxidant enzymes (e.g., superoxide dismutase and catalase to scavenge excess ROS, and accumulating osmoprotectants (e.g., soluble sugars and proline) to maintain intracellular homeostasis and improve cellular water retention [3,17–19].

Roots act as intermediaries in material exchange with soil, where root surfaces serve as the primary interface for the acquisition of metal ions [20]. Soil colloids and root surface both carry permanent and variable charges, derived from the dissociation of functional groups (e.g., carboxyl, hydroxyl, phosphate) that originate from cell wall components including pectin and hemicellulose [21,22]. These surface negative charges not only serve as the initial defense line for ion ingress, but also fundamentally dictate the adsorption of cations (e.g., Cu^{2+}, Mn^{2+}) at the root interface [23,24].

The surface charge of plant roots (characterized by zeta potential) serves as a core factor regulating the adsorption and uptake of metal cations such as Al^{3+} and Cu^{2+} [23,25]. Generally, an increase in the negativity of root zeta potential is accompanied by a marked rise in the capacity to adsorb metal cations [26,27]. Xiang et al. [28] confirmed that the enhanced negative zeta potential of centipedegrass roots correlates tightly with increased densities of functional groups (e.g., carboxylate anions, $-COO^-$), which provide more Al^{3+} binding sites, thus boosting root surface adsorption capacity and elevating root Al^{3+} concentrations. This classic electrochemical principle that "surface charge dictates ion adsorption" can also be extended to the analysis of Na^+ adsorption mechanisms, where Na^+ adsorbed on root surfaces may act as a critical ion pool for its subsequent transmembrane uptake. However, the correlation between root surface charge and plant salt tolerance has not been reported.

Seashore paspalum (*Paspalum vaginatum*) is a perennial grass species with remarkable salt tolerance, rapid growth and low maintenance needs, holding great promise for wide applications in tropical and subtropical regions [29–31]. The salt-tolerant capacity of seashore paspalum is governed by multiple physiological processes, including osmotic regulation [32], K^+/Na^+ homeostasis [31], Na^+ isolation in leaf papillae [33] and hormone regulation [31]. Under salt stress, the K^+ content decreased while the Na^+ content increased in both shoots and roots of seashore paspalum [34]. Variations in salt tolerance among

different seashore paspalum genotypes were closely associated with Na^+ accumulation in roots; specifically, salt-tolerant cultivars tend to accumulate higher levels of Na^+ in roots, compartmentalize excessive Na^+ into vacuoles, and induce the production of hydrogen peroxide in roots, thereby further activating the plant's antioxidant defense system [31,32]. At present, many studies have been conducted on the physiological and molecular regulatory mechanisms underlying the salt tolerance of seashore paspalum shoots. In contrast, studies focusing on the physiological response mechanisms of its roots to salt stress remain limited. However, the relationship between root surface charge characteristics and plant salt tolerance remains largely unexplored.

To address this knowledge gap, two seashore paspalum genotypes with contrasting salt tolerance—the salt-tolerant "Sealsle2000" and the salt-sensitive "17U-45"—were used to characterize root morphological, physiological, and metabolic responses to salt stress, and to reveal the intrinsic correlations among root surface charge, Na^+ adsorption behavior, and salt tolerance. These results will not only deepen our insights into the salt tolerance regulatory network of seashore paspalum, but also offer novel perspectives for elucidating the salt adaptation mechanisms of other plants.

2. Materials and Methods

2.1. Plant Materials

A salt-tolerant genotype (Sealsle2000) and a salt-sensitive genotype (17U-45) were used as experimental materials. These materials were obtained from the Tropical Turfgrass and Forage Germplasm Resource Nursery of Hainan University.

2.2. Experimental Design

The experiment was conducted at the Institute of Botany, Jiangsu Province and the Chinese Academy of Sciences, Nanjing, China (118°46′ E, 32°03′ N) using hydroponic solution culture. Healthy and uniform stolons with the first three nodes were selected and transplanted into polyethylene plastic buckets (17 cm in diameter, 20 cm in height) containing 3.0 L of 1/2 Hoagland nutrient solution. Each bucket was covered with a black polyethylene plate with 16 evenly spaced holes, and one stolon cutting was fixed in each hole to stabilize growth. The buckets were placed in a greenhouse under controlled conditions: photosynthetically active radiation of 200 μmol $m^{-2}s^{-1}$, temperature of 28 ± 3 °C, relative humidity of 65–75%, and a 14/10 h day/night cycle. The nutrient solution was refreshed every five days. After two weeks of cultivation, healthy and uniform plants were selected for salt stress (NaCl) treatment, with the stress concentration set at 300 mM. To mitigate the salt shock effect, the NaCl concentration was gradually increased by 75 mM per day, reaching 300 mM on the 4th day. Seedlings without NaCl addition served as the control group (CK). Each bucket represented one biological replicate, with 4 buckets allocated per treatment. A total of 32 buckets were arranged in a randomized complete block design. During the salt stress period, deionized water was regularly replenished to compensate for water loss due to evaporation and transpiration, maintaining a stable solution volume. On the 4th and 8th days after the salt treatment, plants from each treatment were extracted and washed with distilled water.

For the determination of root morphological traits, biomass, physiological parameters, one plant was randomly sampled from each pot as one biological replicate. One portion of the samples (leaves and roots) was used for phenotypic trait determination, while the other portion was immediately frozen in liquid nitrogen and stored at −80 °C for subsequent physiological index analysis. Additionally, root samples from the control group (CK) were collected on the 8th day of salt treatment to analyze the electrochemical properties of the root surface. For the measurement of root zeta potential, functional group characterization,

Na^+ adsorption and desorption, two plants were randomly collected from each pot and pooled as one biological replicate. Each treatment consisted of four independent biological replicates in total.

2.3. Determination of Root Morphological Parameters and Biomass

Root morphological parameters, including total root length, root surface area, root volume, and average diameter were measured using a root scanning apparatus (STD 4800, EPSON, Markham, ON, Canada) and analyzed with Win RHIZO software (Version 5.0, Regent Instruments, Québec City, QC, Canada). Subsequently, shoot and root samples were deactivated at 105 °C for 20 min, then oven-dried at 80 °C for 48 h to measure the shoot dry weight and root dry weight.

2.4. Determination of Physiological Parameters

The Na^+ and K^+ contents in the shoots and roots were measured using a flame spectrophotometer (GENESIS, EDAX Inc., Mahwah, NJ, USA). The activities of superoxide dismutase and catalase were measured using superoxide dismutase and catalase assay kits (Biobox, Nanjing, China). The malondialdehyde content was measured using malondialdehyde assay kits (Biobox, Nanjing, China). The soluble sugar content was determined following the thiobarbituric acid method [35]. The proline content was measured with a proline assay kit (Biobox, Nanjing, China).

2.5. Determination of Root Zeta Potential

On the 8th day of salt treatment, root samples of the Sealsle2000 and 17U-45 from the control group were harvested. After rinsing with distilled water, the zeta potential of the root was determined via a streaming potential device [36]. Briefly, roots were cut into 2 cm segments, homogenized, and loaded into the sample cell. The storage tank of the apparatus was filled with 1.0 L of NaCl electrolyte solution (conductivity 80 ± 2 μS/cm) and equilibrated for 1.5 h. Then, the solution was replaced with 1.0 L of fresh NaCl electrolyte solution and equilibrated for 5 min before measurement. Five pH gradients were set (pH 6.57, 5.79, 5.12, 4.69, 4.15). Streaming potential (ΔE) was measured using Ag/AgCl electrodes fixed at both ends of the sample cell, while the total conductivity (κ) of the sample was quantified with Pt electrodes at the same positions. An electrolyte solution was pumped into the sample cell with a peristaltic pump, and the valve was adjusted to alter the driving force, thereby obtaining ΔE values under different hydraulic pressure differences (ΔP). The zeta potential of root surfaces was calculated using the Helmholtz–Smoluchowski equation:

$$\zeta = (\Delta E/\Delta P) \times (\mu/\varepsilon\varepsilon_0) \times \kappa$$

where ζ = zeta potential (mV), ΔE = streaming potential (mV), ΔP = liquid pressure difference (Pa), μ = viscosity coefficient of the solution (Pa·s), ε = dielectric constant of the electrolyte solution (F/m), ε_0 = dielectric constant of the vacuum medium (F/m), and κ = solution conductivity (S/m).

2.6. Determination of Na^+ Adsorption and Desorption

Root samples of Sealsle2000 and 17U-45 from the control group were soaked in deionized water for 12 h, with the water renewed every 4 h to thoroughly eliminate residual ions adhering to the root surface. Subsequently, the pre-treated roots were incubated in 300 mmol·L^{-1} NaCl solution for 1 h under magnetic stirring to facilitate Na^+ adsorption. After the adsorption reaction, roots were transferred to 0.1 mol·L^{-1} KNO_3 solution for 0.5 h of desorption, aiming to extract exchangeable Na^+ adsorbed on the root epidermis.

Upon desorption completion, root samples were harvested, deactivated at 105 °C for 30 min, and then oven-dried at 80 °C to a constant weight prior to weighing. The Na^+ content in the desorption solution and the Na^+ content in the root tissues were quantified separately using a flame spectrophotometer.

2.7. Attenuated Total Reflection Infrared Spectroscopy (ATR-FTIR)

Root samples of Sealsle2000 and 17U-45 from the control group were washed with deionized water, air-dried, and analyzed using a Nicolet iS10 infrared spectrometer (Nicolet Analytical Instruments, Madison, WI, USA) equipped with a diamond ATR probe [36]. The spectral scanning range was 400~4000 cm^{-1}, the scanning resolution was 4 cm^{-1}, and the spectral collection for each sample was performed by averaging 32 scans.

2.8. Data Analysis

Experimental data were processed using Microsoft Excel 2021 (Microsoft Corporation, Redmond, WA, USA) and statistically analyzed via SPSS 26.0 (SPSS Inc., Chicago, IL, USA). Data were presented as the mean ± standard error (SE). Normality of distribution and homogeneity of variance were verified using histograms, the Shapiro–Wilk test, and Levene's test, respectively; non-normally distributed data were subjected to logarithmic transformation prior to further analysis. One-way analysis of variance (ANOVA) was employed to evaluate the significant differences among treatment groups at each sampling time point. Post hoc pairwise comparisons were conducted using Duncan's multiple range test to identify specific treatment effects, with significance set at $p < 0.05$. Graphical visualization of data was accomplished using Origin 2025 (OriginLab Corporation, Northampton, MA, USA). Pearson's correlation analysis was performed in SPSS 26.0 to determine the correlation among the measured morphological and physiological parameters.

3. Results

3.1. Effect of Salt Stress on Root Morphological Parameters and Biomass

After 8 days of salt stress treatment, the growth of both genotypes was inhibited. The salt-sensitive genotype (17U-45) exhibited obvious leaf chlorosis and wilting, and their growth was inhibited to a significantly greater extent than that of the salt-tolerant genotype (Sealsle2000) (Figure 1a). Salt stress exerted a prominent inhibitory effect on the growth of seashore paspalum. At 4 days post salt stress, only the root volume of Sealsle2000 was significantly reduced by 11.50% compared with CK, while no statistically significant differences were observed in total root length, root surface area, average diameter, shoot dry weight and root dry weight between salt stress and CK (Figure 1b–h). In contrast, the total root length, root surface area, root volume, average diameter, shoot dry weight and root dry weight of 17U-45 were decreased by 9.25%, 11.21%, 20.93%, 15.37%, 7.93% and 15.00%, respectively, relative to the CK (Figure 1). After 8 days of salt stress exposure, the total root length, root surface area, root volume, average diameter, shoot dry weight and root dry weight of Sealsle2000 were reduced by 6.29%, 10.13%, 12.74%, 11.95%, 12.13% and 13.72%, respectively, compared with the CK, while no significant difference was observed in average diameter between salt stress and CK. For 17U-45, the reduction amplitudes of the above parameters were further exacerbated, with decreases of 18.65%, 17.52%, 21.62%, 22.93%, 27.97% and 39.68% relative to the CK. Salt stress imposed a more severe inhibitory effect on root growth than on the shoot growth of seashore paspalum. Moreover, the reduction extent of all the determined parameters in the salt-sensitive genotype was significantly greater than that in the salt-tolerant genotype.

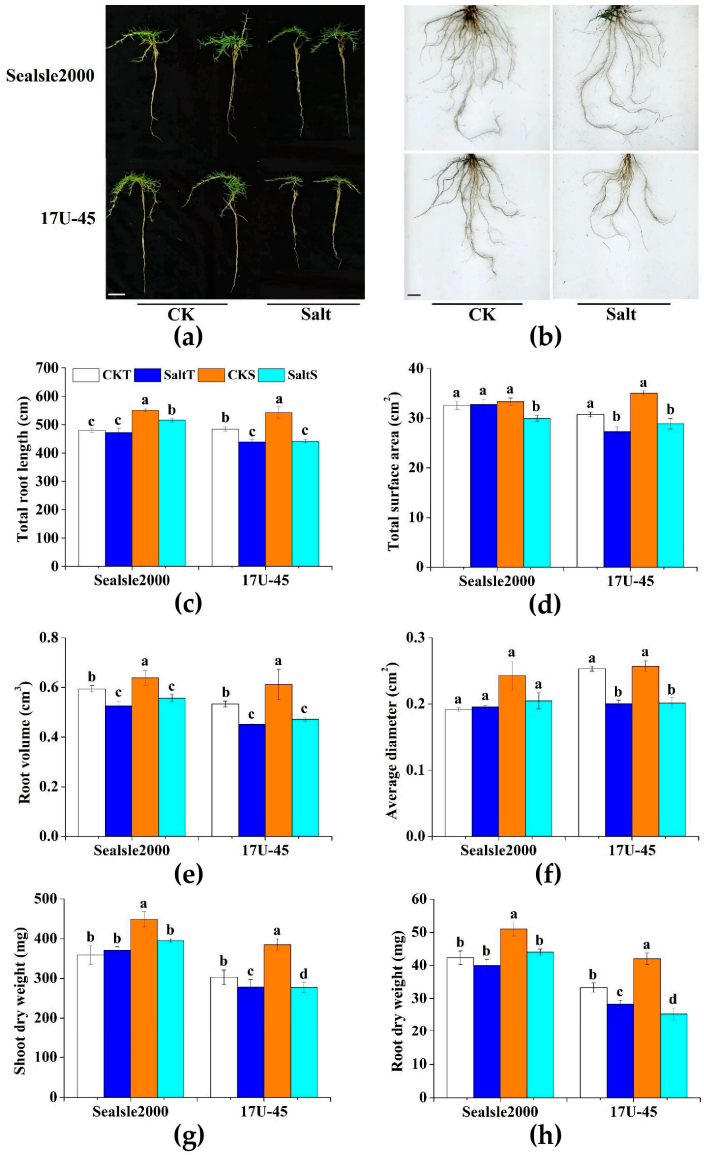


Figure 1. Growth performance of the seashore paspalum (Sealsle2000 and 17-U45) plants under 300 mM NaCl stress. (**a**) Morphology of plants after 8 days of 300 mM NaCl stress, (**b**) root morphology after 8 days of 300 mM NaCl stress, (**c**) total root length, (**d**) total root surface area, (**e**) root volume, (**f**) average diameter treatment, (**g**) shoot dry weight, (**h**) root dry weight after 4 and 8 days of 300 mM NaCl stress. CKT: well water after 4 days of salt treatment, SaltT: 300 mM NaCl treatment for 4 days, CKS: well water after 8 days of salt treatment, SaltS: 300 mM NaCl treatment for 8 days. Error bars indicate the standard error. The presence of distinct lowercase letters on the same day indicates significant differences at the $p < 0.05$ level among all treatments, as determined by Duncan's test. Bar represent 5 cm.

3.2. K^+ and Na^+ Contents and K^+/Na^+ Ratios

Compared with the CK, the accumulation of Na^+ in both the leaves and roots of seashore paspalum increased significantly. Furthermore, with the extension of salt stress duration, the Na^+ accumulation rate in all salt-treated groups was further enhanced (Figure 2a,b). On the 8th day of treatment, the Na^+ contents in leaves and roots of Sealsle2000 increased by 28.13-fold and 36.03-fold, respectively, while those of 17U-45 increased by 18.68-fold and 22.00-fold. The roots of both genotypes exhibited stronger Na^+ enrichment capacity, and the Na^+ accumulation in Sealsle2000 was significantly higher than that in 17U-45 (Figure 2a,b).

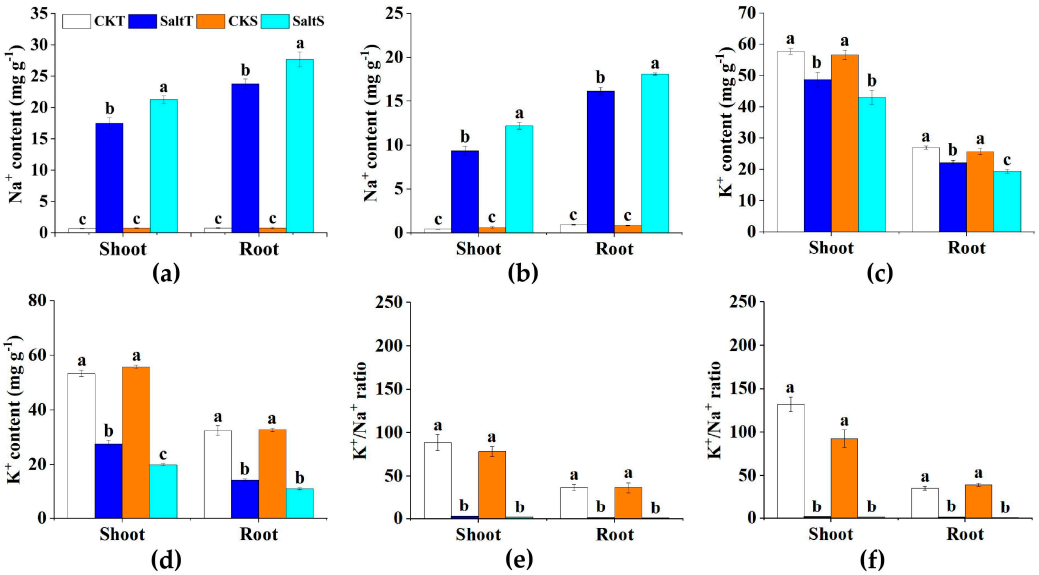


Figure 2. Effects of 300 mM NaCl stress on Na^+ and K^+ contents, K^+/Na^+ ratio in leaves and roots of seashore paspalum (Sealsle2000 and 17-U45) seedlings. (**a**) Na^+ contents in leaves and roots of Sealsle2000, (**b**) Na^+ contents in leaves and roots of 17U-45, (**c**) K^+ contents in leaves and roots of Sealsle2000, (**d**) K^+ contents in leaves and roots of 17U-45, (**e**) K^+/Na^+ ratio in leaves and roots of Sealsle2000, (**f**) K^+/Na^+ ratio in leaves and roots of 17U-45. CKT: well water after 4 days of salt treatment, SaltT: 300 mM NaCl treatment for 4 days, CKS: well water after 8 days of salt treatment, SaltS: 300 mM NaCl treatment for 8 days. Error bars indicate the standard error. The presence of distinct lowercase letters on the same day indicates significant differences at the $p < 0.05$ level among all treatments, as determined by Duncan's test.

In contrast to CK, the K^+ contents in the shoots and roots of both Sealsle2000 and 17U-45 showed a downward trend (Figure 2c,d). On the 4th day of treatment, compared with CK, the K^+ contents in the shoots and roots of Sealsle2000 decreased by 15.66% and 18.07%, respectively, while those of 17U-45 decreased by 50.77% and 56.05%, respectively. On the 8th day of treatment, the reduction amplitudes further expanded: 23.90% and 24.51% for the shoots and roots of Sealsle2000, and 64.26% and 65.91% for those of 17U-45. Regardless of salt stress, the K^+ contents in the shoots were higher than those in roots. Under salt stress, the K^+ contents in all organs of Sealsle2000 were consistently higher than those of 17U-45.

With the prolongation of salt stress duration, the K^+/Na^+ ratios in the shoots and roots of both genotypes decreased continuously (Figure 2e,f). On the 4th day of salt treatment, compared with CK, the K^+/Na^+ ratios in the shoots and roots of Sealsle2000 decreased by 96.86% and 97.41%, respectively, while those of 17U-45 decreased by 98.58% and 97.52%, respectively. On the 8th day of salt treatment, the reduction amplitudes of K^+/Na^+ ratios in the shoots and roots of Sealsle2000 increased to 97.42% and 98.06%, respectively, and those of 17U-45 further expanded to 98.70% and 98.52%, respectively. These results demonstrated that the K^+/Na^+ ratios in the leaves and roots of 17U-45 were lower than those of Sealsle2000, with a more dramatic reduction relative to CK.

3.3. Antioxidant Enzyme Activities, Malondialdehyde Content, and Osmotic Adjustment Substances

With the extension of salt treatment duration, the superoxide dismutase activity in the roots of both Sealsle2000 and 17U-45 exhibited a trend of first increasing and then decreasing (Figure 3a). At 4 days of salt treatment, the root superoxide dismutase activity of Sealsle2000 was significantly increased by 175.19% compared with CK, while that of 17U-45 was elevated by 102.81% relative to CK. At 8 days of salt treatment, the superoxide

dismutase activity of Sealsle2000 remained 68.72% higher than CK. In contrast, the superoxide dismutase activity in 17U-45 decreased by 32.76% relative to the CK, but the difference was not statistically significant. The change trend of catalase activity was consistent with that of superoxide dismutase. As salt treatment prolonged, the root catalase activity of both genotypes first increased and then decreased (Figure 3b). At 4 days of treatment, the root catalase activity of Sealsle2000 and 17U-45 was increased by 91.41% and 26.83% compared with CK, respectively. At 8 days of treatment, the catalase activity of Sealsle2000 still maintained a 65.66% increase relative to CK, while that of 17U-45 was decreased by 36.44% compared with CK.

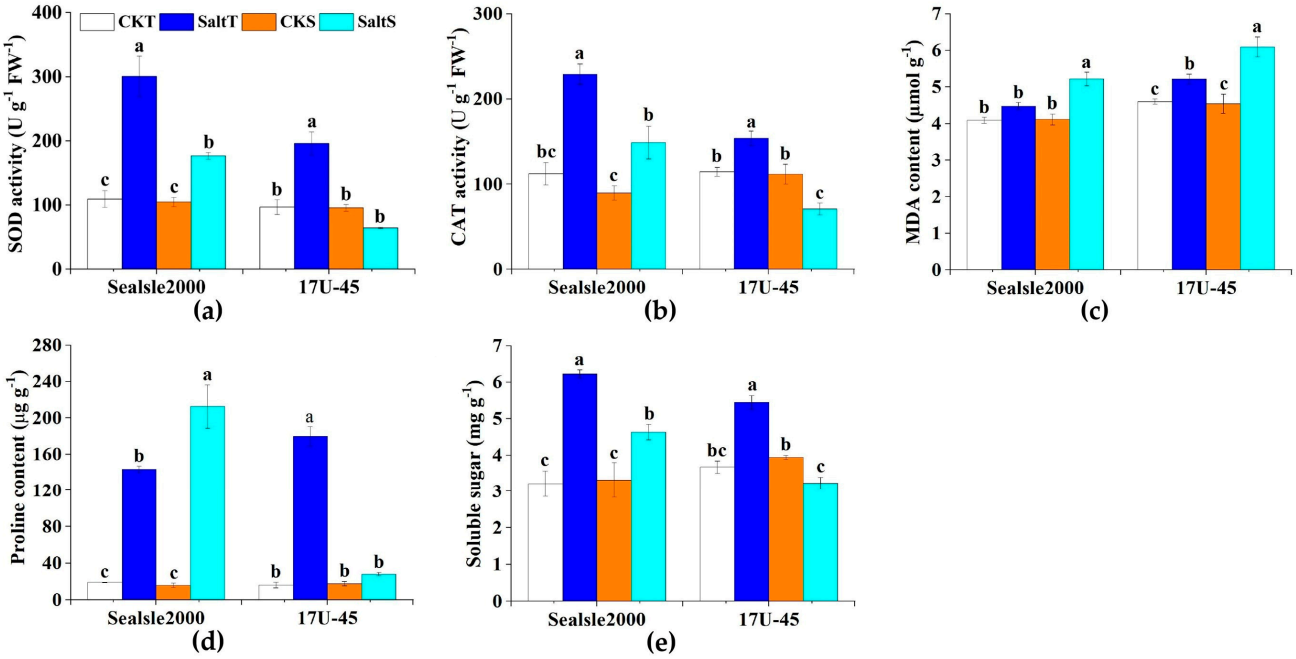


Figure 3. Effects of 300 mM NaCl stress on superoxide dismutase (SOD) (**a**) and catalase (CAT) (**b**) activities, malondialdehyde (MDA) (**c**), proline (**d**) and soluble sugar (**e**) contents in roots of seashore paspalum (Sealsle2000 and 17-U45). CKT: well water after 4 days of salt treatment, SaltT: 300 mM NaCl treatment for 4 days, CKS: well water after 8 days of salt treatment, SaltS: 300 mM NaCl treatment for 8 days. Error bars indicate the standard error. The presence of distinct lowercase letters on the same day indicates significant differences at the $p < 0.05$ level among all treatments, as determined by Duncan's test.

With the prolongation of salt treatment, the malondialdehyde content in the roots of both Sealsle2000 and 17U-45 showed a gradual upward trend (Figure 3c). At 4 and 8 days of salt treatment, the root malondialdehyde content in Sealsle2000 was increased by 9.59% and 26.96% compared with CK, respectively, but the increase at 4 d was not statistically significant. In contrast, that of 17U-45 was elevated by 13.38% and 34.14% relative to CK, respectively, with a more significant increase amplitude. Under salt stress, the root proline content exhibited different change patterns between the two genotypes: The proline content of Sealsle2000 continued to increase with prolonged treatment, while that of 17U-45 first increased and then decreased (Figure 3d). At 4 days of salt treatment, the root proline content of Sealsle2000 and 17U-45 was increased by 6.46-fold and 10.02-fold compared with CK, respectively. At 8 days of treatment, the proline content of Sealsle2000 was further elevated to 12.28-fold that of CK. In contrast, the proline content in 17U-45 was only 0.58-fold higher than the CK, with no significant difference observed, and showed a dramatic decline compared with the 4-day treatment.

The change trend of soluble sugar content in both genotypes was consistent with that of superoxide dismutase and catalase activities, first increasing and then decreasing with the extension of salt treatment (Figure 3e). At 4 days of treatment, the soluble sugar content of both genotypes was significantly higher than that of CK. At 8 days of treatment, the root soluble sugar content of Sealsle2000 remained above the CK level, while that of 17U-45 was significantly lower than CK, indicating a loss of osmotic adjustment capacity in 17U-45 under prolonged salt stress.

3.4. Root Surface Zeta Potential and Na^+ Adsorbed by Roots

Roots of both Sealsle2000 and 17U-45 carried a net negative charge within the pH range of 4.15–6.57, and the absolute value of root zeta potential of seashore paspalum increased with the elevation of solution pH (Figure 4). Within this pH range, the root zeta potential of Sealsle2000 was more negative than that of 17U-45, indicating that Sealsle2000 roots had a higher density of negative charges on their surface compared with 17U-45. In addition, the Na^+ contents on the root surface and in the root tissues of Sealsle2000 were significantly higher than those of 17U-45, with increases of 23.57% and 29.26%, respectively.

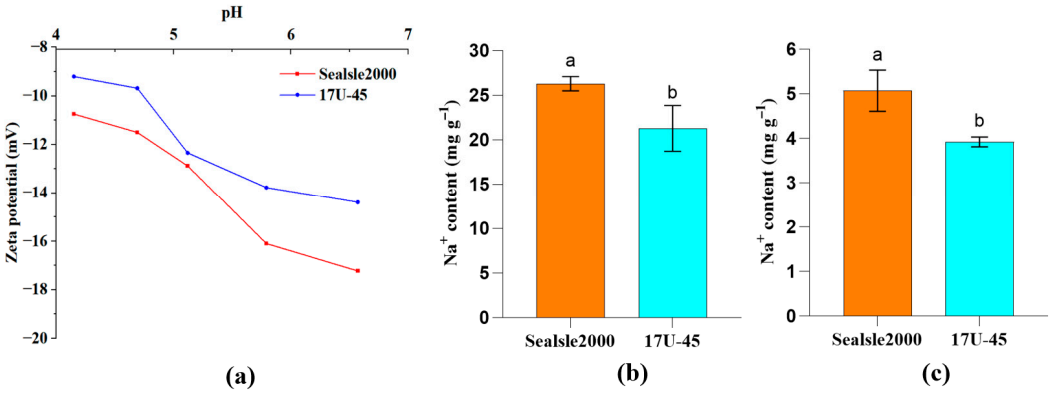


Figure 4. Root zeta potential with solution pH (**a**), root surface Na^+ (**b**) and root interior Na^+ (**c**) of seashore paspalum (Sealsle2000 and 17-U45). Error bars indicate the standard error. The presence of distinct lowercase letters indicates significant differences at the $p < 0.05$ level among all treatments, as determined by Duncan's test.

3.5. Functional Groups on Root Surfaces

ATR-FTIR analysis of root surface functional groups showed no significant difference in absorption peak positions between Sealsle2000 and 17U-45 (Figure 5), indicating that their root surfaces contain similar functional groups. Specific absorption peaks and their corresponding functional groups are as follows: The peak at 1729 cm^{-1} is associated with C=O stretching vibrations of non-conjugated carbonyl groups in lignin and ester groups in hemicellulose; the peak at 1637 cm^{-1} relates to the conjugated carbonyl structure of lignin, including planar vibrations of aromatic ring C=C; the peak at 1513 cm^{-1} corresponds to C=C stretching vibrations in the aromatic ring skeleton of lignin; the peak at 1384 cm^{-1} is linked to C-H bending vibrations in cellulose and hemicellulose; the peak at 1255 cm^{-1} originates from acyloxy bond (CO-OR) stretching vibrations in hemicellulose, possibly accompanied by the mixed absorption of partial benzene ring C-H stretching vibrations; and the peak at 1047 cm^{-1} is mainly attributed to C-O and C-O-C stretching vibrations in cellulose and hemicellulose. Notably, the absorption peak intensities of the Sealsle2000 were higher than those of the 17U-45, suggesting that the root surfaces of salt-tolerant seashore paspalum contain more functional groups.

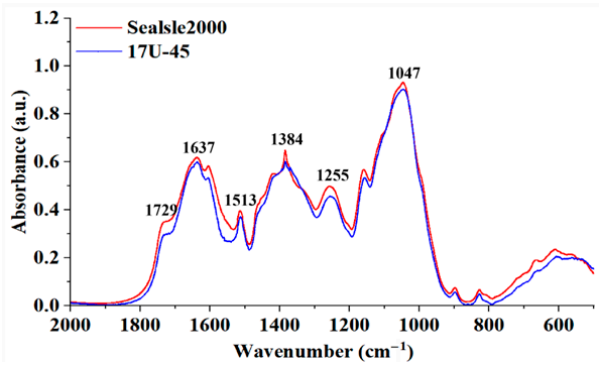


Figure 5. FTIR spectra of root surfaces from seashore paspalum (Sealsle2000 and 17-U45).

3.6. Relationship Between Morphological, Physiological Parameters and Surface Charge

Correlation analysis was performed on the measured root traits of seashore paspalum in both treatment and control groups (Figure 6). The results revealed that shoot Na^+ content, root Na^+ content, root surface Na^+ and internal root Na^+ exhibited significant negative correlations with root morphological and plant growth parameters. In contrast, shoot K^+ content, root K^+ content, shoot K^+/Na^+ ratio and root K^+/Na^+ ratio were positively correlated with these morphological and growth parameters. Root malondialdehyde content was negatively correlated with all the tested morphological and growth parameters, with the exception of average diameter. Additionally, root surface zeta potential was positively correlated with total surface area, root volume, average diameter, shoot K^+/Na^+ ratio and root K^+/Na^+ ratio, but negatively correlated with shoot Na^+ content and root Na^+ content.

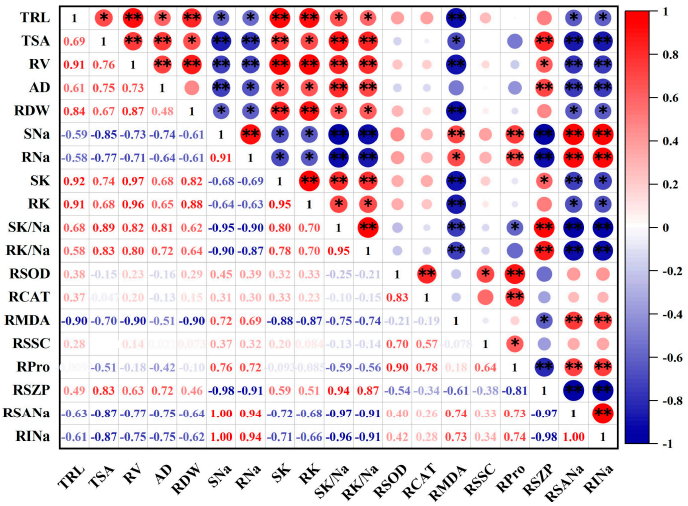


Figure 6. Correlation coefficients among morphological, physiological index and root surface electrochemical traits of seashore paspalum (Sealsle2000 and 17-U45) under 300 mM NaCl stress. TRL: total root length, TSA: total surface area, RV: root volume, AD: average diameter, RDW: root dry weight, SNa: shoot Na^+ content, RNa: root Na^+ content, SK: shoot K^+ content, RK: root K^+ content, SK/Na: shoot K^+/Na^+ ratio, RK/Na: root K^+/Na^+ ratio, RSOD: root SOD activity, RCAT: root CAT activity, RMDA: root MDA content, RSSC: root soluble sugar content, RPro: root proline content, RSZP: root surface zeta potential, RSANa: root surface Na^+, RINa: root interior Na^+. The difference in colors represent significance difference at $p < 0.05$, red color represents positive correlation, and blue color represents negative correlation. * $p < 0.05$, ** $p < 0.01$.

4. Discussion

As a typical halophytic herbaceous plant, seashore paspalum possesses considerable application potential in the vegetation reconstruction of saline–alkali soils due to its ex-

cellent salt tolerance. As the primary organ for plants to perceive soil salinity signals, the morphological remodeling and adaptive regulation of physiological metabolism in roots constitute the core basis of plant salt tolerance [8,10,13]. In this study, we systematically characterized the morphological traits, physiological parameters, and surface charge properties of seashore paspalum roots under salt stress, which provides critical theoretical insights for an in-depth understanding of its salt tolerance regulatory mechanisms.

4.1. Root Morphological Adaptations to Salt Stress

As the first organ to contact and perceive salt stress, roots have evolved a range of morphological structures to adapt to salt stress [3,9,37]. The extent of the effect of salt treatment on root growth is significantly dependent on stress intensity [8]. This study revealed that the impacts of salt stress on the shoot and root growth of seashore paspalum exhibited significant genotypic differences and time-dependent characteristics. Short-term salt stress (4 days) exerted no significant effect on shoot and root growth in the salt-tolerant genotype, with the exception of root volume, whereas it significantly inhibited growth in the salt-sensitive genotype. With stress prolonged to 8 days, both genotypes were significantly inhibited; however, the salt-tolerant genotype was less affected than the salt-sensitive one, and root growth was inhibited more severely than shoot growth. The inhibition of root growth impairs the plant's ability to absorb water and essential mineral nutrients, thereby reducing their supply to shoots, which may be an important reason for the inhibition of overall growth of seashore paspalum, especially in salt-sensitive genotypes [38]. Under salt stress, the salt-tolerant genotype Sealsle2000 maintained more stable root growth and suffered milder inhibition than the salt-sensitive 17U-45, especially during the early stage of stress. With prolonged salt stress, root growth in both genotypes was inhibited, but the reduction was less pronounced in Sealsle2000 than in 17U-45. This stronger root stability helps to maintain water and nutrient uptake under salt stress, thus alleviating growth inhibition.

4.2. Ion Homeostasis Regulation Under Salt Stress

Maintaining intracellular Na^+/K^+ homeostasis is a core physiological mechanism underlying plant salt tolerance, and the selective absorption and compartmentalized distribution of ions by roots directly determine their salt tolerance capacity [39,40]. High salt (NaCl) stress induces excessive accumulation of Na^+ and Cl^- at both the cellular and whole-plant levels [3,41]. In this study, the shoot and root Na^+ contents of both genotypes increased significantly with escalating salt stress intensity. However, Sealsle2000 accumulated a higher level of Na^+ than 17U-45, and root Na^+ content was significantly higher than that in shoots. This observation is consistent with the findings of Lee et al. [42], who reported that salt stress increases Na^+ contents in both the shoots and roots of seashore paspalum. A similar phenomenon of higher root Na^+ content than shoot content has also been reported in olive trees [43]. It is speculated that Sealsle2000 can preferentially accumulate absorbed Na^+ in roots and compartmentalize it into root cell vacuoles by maintaining a superior root architecture. This strategy reduces Na^+ translocation to the shoot, mitigating the inhibitory effect of ionic toxicity on physiological processes such as photosynthesis, hormone metabolism, and carbon assimilation [39,44–46]. Existing studies have confirmed that plant salt tolerance is closely related to the ability of roots to retain salt ions and prevent Na^+ accumulation in shoots [4,37].

K^+ acts as a pivotal osmoregulatory ion in plant cells, participating in the regulation of stomatal movement, the sustainment of photosynthetic activity, the stabilization of ion homeostasis, and the mitigation of oxidative damage under adverse conditions [3,4,47–49]. Moreover, the ability to maintain K^+ homeostasis is recognized as a crucial factor in

alleviating Na^+ toxicity under salt stress [4]. In this study, shoot and root K^+ contents of both genotypes gradually decreased with the extension of salt stress duration, showing a distinct time-dependent effect, and the reduction amplitude in roots was greater than that in shoots. Notably, the decrease in shoot and root K^+ contents of Sealsle2000 was smaller than that of 17U-45, which might be attributed to its superior root morphology and consequent water and nutrient absorption capacity.

During salt stress, plants counterbalance the elevated Na^+ contents by maintaining K^+ contents in tissues, thereby sustaining a higher K^+/Na^+ ratio to prevent cellular damage and nutrient deficiency [50,51]. This study showed that the K^+/Na^+ ratios of both Sealsle2000 and 17U-45 decreased significantly under salt stress, indicating potential disturbances in osmotic balance and cellular metabolism. Nevertheless, the reduction amplitude of the K^+/Na^+ ratio in Sealsle2000 was lower than that in 17U-45, suggesting that Sealsle2000 can preserve normal cellular physiological functions by minimizing K^+ loss and retaining a relatively high K^+/Na^+ ratio. Similar salt stress-triggered reductions in the K^+/Na^+ ratio have been observed in kiwifruit [4] and black walnut [3], where salt-tolerant genotypes showed less pronounced decreases compared to salt-sensitive lines.

4.3. Antioxidant System and Osmotic Adjustment Under Salt Stress

Salt stress induces the accumulation of reactive oxygen species, triggering oxidative stress that disrupts membrane lipids, denatures proteins, and causes severe cellular damage or death [3,4]. To mitigate damage caused by excessive reactive oxygen species, plants have evolved enzymatic and non-enzymatic reactive oxygen species scavenging mechanisms [18]. Superoxide dismutase and catalase are key enzymes in plant reactive oxygen species scavenging systems [51,52]. In this study, the superoxide dismutase and catalase activities of 17U-45 were higher than those of the control (CK) under short-term salt stress but decreased significantly in the later stage. This may be due to the inhibition of the antioxidant enzyme synthesis system in 17U-45 under long-term salt stress, or the damage to enzyme structure by excessive reactive oxygen species, leading to the collapse of its antioxidant defense system and ineffective reactive oxygen species scavenging. In contrast, the superoxide dismutase and catalase activities of Sealsle2000 increased significantly under salt stress and remained at a high level even after 8 days of treatment. These results indicate that Sealsle2000 can scavenge reactive oxygen species by activating superoxide dismutase and catalase, thereby alleviating long-term salt-induced oxidative damage and sustaining a relatively high rate of root growth. This finding aligns with previous reports on rice [52], maize [53], and black walnut [3], where salt-tolerant genotypes preserved vigorous growth by maintaining elevated superoxide dismutase and catalase activities.

Malondialdehyde, the product of membrane lipid peroxidation [17], accumulated continuously in the roots of both genotypes with extended salt treatment, but the increment was significantly higher in 17U-45. This higher malondialdehyde accumulation reflected more severe membrane oxidative damage in 17U-45, which was closely linked to reduced antioxidant enzyme activities and impaired reactive oxygen species scavenging capacity under long-term stress. By comparison, Sealsle2000 exhibited relatively low malondialdehyde accumulation, implying superior membrane structural integrity derived from its sustained high antioxidant enzyme activities.

In addition to antioxidant defense, the accumulation of osmotic adjustment substances represents another key strategy for plants to combat salt-induced osmotic damage [54]. Proline and soluble sugar stabilize enzymes and proteins, protect membrane integrity, and alleviate osmotic stress-induced impairments to cellular structures and physiological metabolism [4,55]. Studies have shown increased proline and soluble sugar contents under increasing salt stress, while a decrease in these osmolytes has been observed under

extremely high salt concentrations or prolonged stress [3,17,56,57]. This discrepancy may stem from differential responses of various organic osmolytes to salt stress, potentially linked to their differing contributions to osmotic adjustment [58]. Under salt stress, the roots of both Sealsle2000 and 17U-45 accumulated proline and soluble sugar, but Sealsle2000 exhibited more sustained osmotic adjustment capacity. These results indicate that Sealsle2000 sustains the synthesis of osmotic adjustment substances to maintain osmotic balance, ensuring normal water uptake and cellular metabolism. Conversely, 17U-45 has limited osmotic adjustment capacity, failing to effectively counteract long-term salt-induced osmotic stress and ultimately leading to impaired physiological functions and inhibited growth.

4.4. Correlation Between Root Electrochemical Traits and Salt Tolerance

The dissociation of functional groups on the plant root surface confers negative charge traits on the root system, and this electrochemical feature directly regulates the adsorption and absorption of metal cations by roots [25,59]. Previous studies have confirmed a marked positive correlation between the negativity of root zeta potential and cation adsorption capacity: A more negative zeta potential corresponds to stronger root adsorption of cations such as aluminum (Al^{3+}) [23], manganese (Mn^{2+}) [59], and cadmium (Cd^{2+}) [25]. In this study, salt-tolerant seashore paspalum exhibited a more negative root zeta potential, which facilitated greater adsorption and uptake of Na^+. Our results are consistent with those reported by Xiang et al. [28] in the perennial grass centipedegrass, where provenances with a more negative root surface potential adsorbed and absorbed more Al^{3+}. Likewise, our findings agree with those of Liu et al. [23] in rice, in which varieties with a more negative root zeta potential showed enhanced root adsorption and absorption of Al^{3+}. ATR-FTIR spectral analysis revealed that the types of functional groups on the root surface were basically consistent between Sealsle2000 and 17U-45, while the concentration of specific charge-bearing groups (e.g., non-conjugated carbonyl groups at 1729 cm^{-1}) was higher in Sealsle2000. The structural and content features of these charge-bearing groups provide a key physicochemical basis for the observed differences in root zeta potential between the two genotypes [21,22]. Collectively, our results indicate that the salt tolerance of Sealsle2000 is associated with variations in root cell wall structure and composition, rather than the presence or absence of specific functional groups.

5. Conclusions

Salt stress suppressed shoot and root growth, altered root morphology, and disrupted the physiological metabolism in both Sealsle2000 and 17U-45, but marked differences in their salt tolerance responses were observed (Figure 7). Overall, 17U-45 exhibited higher salt sensitivity, as its growth and physiological metabolism were more severely inhibited by salt stress. In contrast, Sealsle2000 enhanced salt tolerance via the multi-pathway synergistic regulation verified in this study: modifying root architecture to increase root length and surface area; expanding the absorption area; elevating antioxidant enzyme activities to scavenge reactive oxygen species accumulation; increasing osmotic adjustment substance contents to maintain cellular osmotic balance; and promoting selective root K^+ uptake while sustaining a high K^+/Na^+ ratio, thereby preserving intracellular homeostasis and cell membrane stability. Additionally, the higher concentration of specific charged groups in Sealsle2000 contributes to a more negative root surface zeta potential, which promotes root Na^+ uptake, facilitates vacuolar Na^+ sequestration, reduces cytoplasmic Na^+ toxicity, and further alleviates salt-induced plant damage. Future research should focus on exploring salt tolerance-related molecular mechanisms, specifically clarifying the molecular pathways linking root surface charge to salt tolerance.

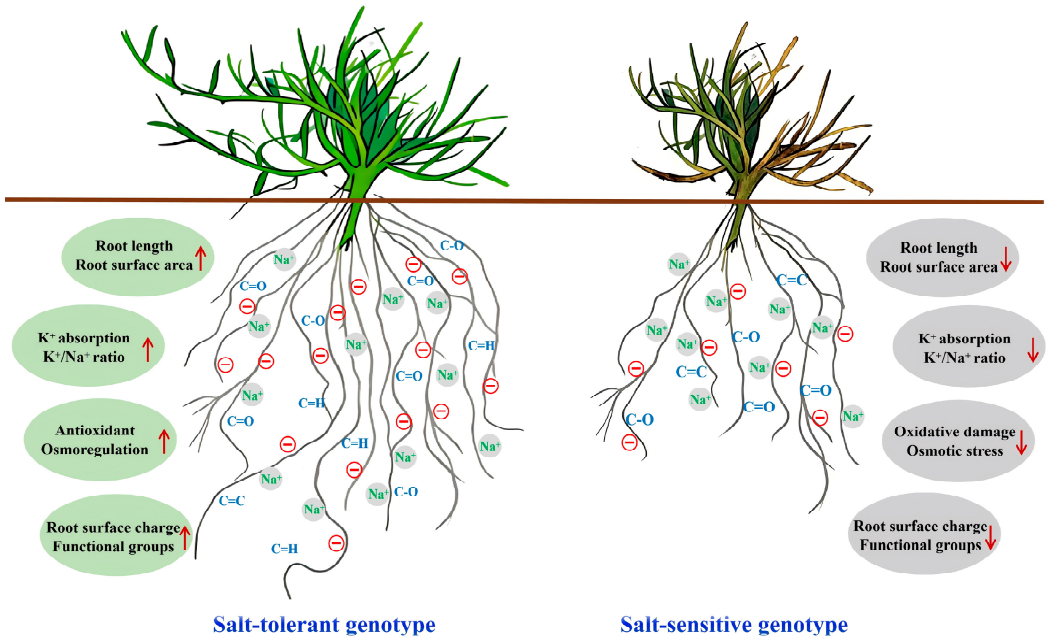


Figure 7. Schematic diagram of root responses to salt stress in salt-tolerant and salt-sensitive genotypes of seashore paspalum. Arrows (↑/↓) show changes under salt stress, ↑ increase, ↓ decrease; Gray lines: roots; Blue labels (C=O, C-O, C-H, C=C, etc.): root surface functional groups; Na^+ (gray circles): sodium ions; Red circles (⊖): root surface negative charges.

Author Contributions: Conceptualization, S.Y. and X.X.; methodology, S.Y., H.L. and D.H.; software, Z.L. and D.H.; investigation, S.Y. and Z.L.; data curation, S.Y. and L.L. (Ling Li); writing—original draft preparation, S.Y.; writing—review and editing, L.L. (Ling Li), Z.W., J.Z. and L.L. (Li Liao); visualization, S.Y. and Z.L.; funding acquisition, Z.W. and L.L. (Li Liao). All authors have read and agreed to the published version of the manuscript.

Funding: This research was funded by the National Nature Science Foundation of China (32371782, 32460358), and Hainan Provincial Science and Technology Talent Innovation Fund Project (KJRC2023C21).

Data Availability Statement: The original contributions presented in this study are included in the article. Further inquiries can be directed to the corresponding author.

Conflicts of Interest: The authors declare no conflicts of interest.

References

1. Food and Agriculture Organization of the United Nations. *Global Status of Salt-Affected Soils*; Food and Agriculture Organization of the United Nations: Rome, Italy, 2024. [CrossRef]
2. Gu, J.; Hu, B.; Jia, Y.; Sha, H.; Li, J.; Ma, C.; Zhao, H. Effects of Salt Stress on Rice Root Related Traits and Yield. *Crops* **2019**, *4*, 176–182. (In Chinese) [CrossRef]
3. Ji, X.; Tang, J.; Zheng, X.; Li, A.; Zhang, J. The regulating mechanism of salt tolerance of black walnut seedlings was revealed by the physiological and biochemical integration analysis. *Plant Physiol. Biochem.* **2024**, *210*, 108548. [CrossRef] [PubMed]
4. Abid, M.; Zhang, Y.J.; Li, Z.; Bai, D.F.; Zhong, Y.P.; Fang, J.B. Effect of salt stress on growth, physiological and biochemical characters of four kiwifruit genotypes. *Sci. Hortic.* **2020**, *271*, 109473. [CrossRef]
5. Mishra, A.; Tanna, B. Halophytes: Potential resources for salt stress tolerance genes and promoters. *Front. Plant Sci.* **2017**, *8*, 829. [CrossRef]
6. Sun, S.; Wang, Y.; Wang, J.; Tan, M.; Yan, H.; So, K.; Zhang, Y. Transcriptome responses to salt stress in roots and leaves of Lilium pumilum. *Sci. Hortic.* **2023**, *309*, 111622. [CrossRef]
7. Machado, R.M.A.; Serralheiro, R.P. Soil Salinity: Effect on vegetable crop growth. management practices to prevent and mitigate soil salinization. *Horticulturae* **2017**, *3*, 30. [CrossRef]

8. Zou, Y.; Zhang, Y.; Testerink, C. Root dynamic growth strategies in response to salinity. *Plant Cell Environ.* **2022**, *45*, 695–704. [CrossRef] [PubMed]
9. Dinneny, J.R. Developmental responses to water and salinity in root systems. *Annu. Rev. Cell Dev. Biol.* **2019**, *35*, 239–257. [CrossRef] [PubMed]
10. Julkowska, M.M.; Koevoets, I.T.; Mol, S.; Hoefsloot, H.; Feron, R.; Tester, M.A.; Keurentjes, J.J.; Korte, A.; Haring, M.A.; de Boer, G.-J. Genetic components of root architecture remodeling in response to salt stress. *Plant Cell* **2017**, *29*, 3198–3213. [CrossRef]
11. Korver, R.A.; van den Berg, T.; Meyer, A.J.; Galvan-Ampudia, C.S.; Ten Tusscher, K.H.; Testerink, C. Halotropism requires phospholipase Dζ1-mediated modulation of cellular polarity of auxin transport carriers. *Plant Cell Environ.* **2020**, *43*, 143–158. [CrossRef]
12. Julkowska, M.M.; Hoefsloot, H.C.; Mol, S.; Feron, R.; de Boer, G.-J.; Haring, M.A.; Testerink, C. Capturing Arabidopsis root architecture dynamics with ROOT-FIT reveals diversity in responses to salinity. *Plant Physiol.* **2014**, *166*, 1387–1402. [CrossRef] [PubMed]
13. Li, H.; Duijts, K.; Pasini, C.; van Santen, J.E.; Lamers, J.; de Zeeuw, T.; Verstappen, F.; Wang, N.; Zeeman, S.C.; Santelia, D. Effective root responses to salinity stress include maintained cell expansion and carbon allocation. *New Phytol.* **2023**, *238*, 1942–1956. [CrossRef] [PubMed]
14. Liu, H.; Todd, J.L.; Luo, H. Turfgrass salinity stress and tolerance—A review. *Plants* **2023**, *12*, 925. [CrossRef] [PubMed]
15. Mittova, V.; Guy, M.; Tal, M.; Volokita, M. Salinity up-regulates the antioxidative system in root mitochondria and peroxisomes of the wild salt-tolerant tomato species *Lycopersicon pennellii*. *J. Exp. Bot.* **2004**, *55*, 1105–1113. [CrossRef] [PubMed]
16. Liu, C.; Jiang, X.; Yuan, Z. Plant responses and adaptations to salt stress: A review. *Horticulturae* **2024**, *10*, 1221. [CrossRef]
17. Hu, D.; Li, R.; Dong, S.; Zhang, J.; Zhao, B.; Ren, B.; Ren, H.; Yao, H.; Wang, Z.; Liu, P. Maize (*Zea mays* L.) responses to salt stress in terms of root anatomy, respiration and antioxidative enzyme activity. *BMC Plant Biol.* **2022**, *22*, 602. [CrossRef]
18. Qi, J.; Wang, J.; Gong, Z.; Zhou, J.-M. Apoplastic ROS signaling in plant immunity. *Curr. Opin. Plant Biol.* **2017**, *38*, 92–100. [CrossRef]
19. Hao, S.; Wang, Y.; Yan, Y.; Liu, Y.; Wang, J.; Chen, S. A review on plant responses to salt stress and their mechanisms of salt resistance. *Horticulturae* **2021**, *7*, 132. [CrossRef]
20. DiToppi, L.S.; Lambardi, M.; Pecchion, N.; Pazzagli, L.; Durante, M.; Gabbrielli, R. Effects of cadmium stress on hairy roots of Daucus carota. *J. Plant Physiol.* **1999**, *154*, 385–391. [CrossRef]
21. Sharifi, M.; Khoshgoftarmanesh, A.; Hadadzadeh, H. Changes in the chemical properties and swelling coefficient of alfalfa root cell walls in the presence of toluene as a toxic agent. *Environ. Sci. Pollut. Res.* **2016**, *23*, 7022–7031. [CrossRef]
22. Wang, W.; Zhao, X.Q.; Chen, R.F.; Dong, X.Y.; Lan, P.; Ma, J.F.; Shen, R.F. Altered cell wall properties are responsible for ammonium-reduced aluminium accumulation in rice roots. *Plant Cell Environ.* **2015**, *38*, 1382–1390. [CrossRef] [PubMed]
23. Liu, Z.; Wang, H.; Xu, R.K. The effects of root surface charge and nitrogen forms on the adsorption of aluminum ions by the roots of rice with different aluminum tolerances. *Plant Soil* **2016**, *408*, 43–53. [CrossRef]
24. Lu, H.; Liu, Z.; Zhou, Q.; Xu, R.-K. Zeta potential of roots determined by the streaming potential method in relation to their Mn (II) sorption in 17 crops. *Plant Soil* **2018**, *428*, 241–251. [CrossRef]
25. Biswash, M.R.; Lu, H.; Dong, G.; He, X.; Li, J.; Xu, R. Effect of root surface charge on the absorption and accumulation of Cu (II) by different japonica and indica rice varieties under acidic conditions. *Ecotoxicol. Environ. Saf.* **2021**, *223*, 112547. [CrossRef] [PubMed]
26. Dong, G.; Nkoh, J.; Hong, Z.; Dong, Y.; Lu, H.; Yang, J.; Pan, X.; Xu, R. Phytotoxicity of Cu^{2+} and Cd^{2+} to the roots of four different wheat cultivars as related to charge properties and chemical forms of the metals on whole plant roots. *Ecotoxicol. Environ. Saf.* **2020**, *196*, 110545. [CrossRef]
27. Lu, H.; Nkoh, J.; Xu, R.; Dong, G.; Li, J. More negative charges on roots enhanced manganese (II) uptake in leguminous and non-leguminous poaceae crops. *J. Sci. Food Agric.* **2023**, *103*, 3531–3539. [CrossRef]
28. Xiang, X.; Zong, J.; Li, L.; Nkoh, J.N.; Hao, D.; Lu, H. Modulation of root surface charge and functional groups as a key mechanism of aluminum tolerance in centipedegrass (*Eremochloa ophiuroides* [Munro] Hack.). *Plant Physiol. Biochem.* **2025**, *229*, 110673. [CrossRef]
29. Wu, X.; Shi, H.; Guo, Z. Overexpression of a *NF-YC* gene results in enhanced drought and salt tolerance in transgenic seashore paspalum. *Front. Plant Sci.* **2018**, *9*, 1355. [CrossRef]
30. Li, Y.; Yang, Q.; Huang, H.; Guo, Y.; Sun, Q.; Guo, Z.; Shi, H. Overexpression of *PvWAK3* from seashore paspalum increases salt tolerance in transgenic Arabidopsis via maintenance of ion and ROS homeostasis. *Plant Physiol. Biochem.* **2024**, *207*, 108337. [CrossRef]
31. Pan, L.; Xu, T.; Wang, J.; Zhao, J.; Sun, Q.; Hu, X.; Tao, X.; Zhang, J.; Liao, L.; Wang, Z. Root-sourced H_2O_2 is essential for maintaining jasmonic acid and Na^+/K^+ homeostasis to delay leaf senescence during salt stress in Paspalum vaginatum. *Hortic. Plant J.* **2025**, *11*, 1364–1376. [CrossRef]

32. Guo, H.; Wang, Y.; Li, D.; Chen, J.; Zong, J.; Wang, Z.; Chen, X.; Liu, J. Growth response and ion regulation of seashore paspalum accessions to increasing salinity. *Environ. Exp. Bot.* **2016**, *131*, 137–145. [CrossRef]
33. Spiekerman, J.J.; Devos, K.M. The halophyte seashore paspalum uses adaxial leaf papillae for sodium sequestration. *Plant Physiol.* **2020**, *184*, 2107–2119. [CrossRef] [PubMed]
34. Dudeck, A.E.; Peacock, C.H. Effects of salinity on seashore paspalum turfgrasses. *Agron. J.* **1985**, *77*, 47–50. [CrossRef]
35. Zheng, Y.; Jia, A.; Ning, T.; Xu, J.; Li, Z.; Jiang, G. Potassium nitrate application alleviates sodium chloride stress in winter wheat cultivars differing in salt tolerance. *J. Plant Physiol.* **2008**, *165*, 1455–1465. [CrossRef] [PubMed]
36. Lu, H.; Dong, G.; Hua, H.; Zhao, W.; Li, J.; Xu, R. Method for initially selecting Al-tolerant rice varieties based on the charge characteristics of their roots. *Ecotoxicol. Environ. Saf.* **2020**, *187*, 109813. [CrossRef] [PubMed]
37. Aparicio-Durán, L.; Hervalejo, A.; Calero-Velázquez, R.; Arjona-López, J.M.; Arenas-Arenas, F.J. Salinity effect on plant physiological and nutritional parameters of new Huanglongbing disease-tolerant citrus rootstocks. *Agronomy* **2021**, *11*, 653. [CrossRef]
38. Liu, C.; Zhao, X.; Yan, J.; Yuan, Z.; Gu, M. Effects of salt stress on growth, photosynthesis, and mineral nutrients of 18 pomegranate (*Punica granatum*) cultivars. *Agronomy* **2019**, *10*, 27. [CrossRef]
39. Van Zelm, E.; Zhang, Y.; Testerink, C. Salt tolerance mechanisms of plants. *Annu. Rev. Plant Biol.* **2020**, *71*, 403–433. [CrossRef]
40. Abbas, A.; Mansha, S.; Waheed, H.; Siddiq, Z.; Hayyat, M.U.; Zhang, Y.-J.; Alwutayd, K. NaCl stress, tissue specific Na^+ and K^+ up-take and their effect on growth and physiology of *Helianthus annuus* L. and *Solanum lycopersicum* L. *Sci. Hortic.* **2024**, *326*, 112454. [CrossRef]
41. Liu, X.; Zhang, H.; Jin, Y.; Wang, M.; Yang, H.; Ma, H.; Jiang, C.; Liang, Z. Abscisic acid primes rice seedlings for enhanced tolerance to alkaline stress by upregulating antioxidant defense and stress tolerance-related genes. *Plant Soil* **2019**, *438*, 39–55. [CrossRef]
42. Lee, G.J.; Duncan, R.R.; Carrow, R.N. Nutrient uptake responses and inorganic ion contribution to solute potential under salinity stress in halophytic seashore paspalums. *Crop Sci.* **2007**, *47*, 2504–2512. [CrossRef]
43. Kchaou, H.; Larbi, A.; Gargouri, K.; Chaieb, M.; Morales, F.; Msallem, M. Assessment of tolerance to NaCl salinity of five olive cultivars, based on growth characteristics and Na^+ and Cl^- exclusion mechanisms. *Sci. Hortic.* **2010**, *124*, 306–315. [CrossRef]
44. Bose, J.; Munns, R.; Shabala, S.; Gilliham, M.; Pogson, B.; Tyerman, S.D. Chloroplast function and ion regulation in plants growing on saline soils: Lessons from halophytes. *J. Exp. Bot.* **2017**, *68*, 3129–3143. [CrossRef] [PubMed]
45. Mahajan, M.; Poor, P.; Kaur, H.; Aher, R.R.; Palakolanu, S.R.; Khan, M.I.R. Salt stress tolerance and abscisic acid in plants: Associating role of plant growth regulators and transcription factors. *Plant Physiol. Biochem.* **2025**, *228*, 110303. [CrossRef]
46. Wu, P.; Cogill, S.; Qiu, Y.; Li, Z.; Zhou, M.; Hu, Q.; Chang, Z.; Noorai, R.E.; Xia, X.; Saski, C. Comparative transcriptome profiling provides insights into plant salt tolerance in seashore paspalum (*Paspalum vaginatum*). *BMC Genom.* **2020**, *21*, 131. [CrossRef]
47. Ahanger, M.; Agarwal, R. Salinity stress induced alterations in antioxidant metabolism and nitrogen assimilation in wheat (*Triticum aestivum* L) as influenced by potassium supplementation. *Plant Physiol. Biochem.* **2017**, *115*, 449–460. [CrossRef]
48. Che, Y.; Yao, T.; Wang, H.; Wang, Z.; Zhang, H.; Sun, G.; Zhang, H. Potassium ion regulates hormone, Ca^{2+} and H_2O_2 signal transduction and antioxidant activities to improve salt stress resistance in tobacco. *Plant Physiol. Biochem.* **2022**, *186*, 40–51. [CrossRef]
49. Karimi, R.; Ebrahimi, M.; Amerian, M. Abscisic acid mitigates NaCl toxicity in grapevine by influencing phytochemical compounds and mineral nutrients in leaves. *Sci. Hortic.* **2021**, *288*, 110336. [CrossRef]
50. Ren, Z.; Gao, J.; Li, L.; Cai, X.; Huang, W.; Chao, D.; Zhu, M.; Wang, Z.; Luan, S.; Lin, H. A rice quantitative trait locus for salt tolerance encodes a sodium transporter. *Nat. Genet.* **2005**, *37*, 1141–1146. [CrossRef]
51. Zhang, X.; Li, S.; Tang, T.; Liu, Y.; Tahir, M.M.; Wang, C.; Meng, Z.; Niu, J.; Yang, W.; Ma, J. Comparison of morphological, physiological, and related-gene expression responses to saline-alkali stress in eight apple rootstock genotypes. *Sci. Hortic.* **2022**, *306*, 111455. [CrossRef]
52. Challabathula, D.; Analin, B.; Mohanan, A.; Bakka, K. Differential modulation of photosynthesis, ROS and antioxidant enzyme activities in stress-sensitive and-tolerant rice cultivars during salinity and drought upon restriction of COX and AOX pathways of mitochondrial oxidative electron transport. *J. Plant Physiol.* **2022**, *268*, 153583. [CrossRef]
53. Azevedo, A.; Prisco, J.; Enéas-Filho, J.; Abreu, C.; Gomes-Filho, E. Effect of salt stress on antioxidative enzymes and lipid peroxidation in leaves and roots of salt-tolerant and salt-sensitive maize genotypes. *Environ. Exp. Bot.* **2006**, *56*, 87–94. [CrossRef]
54. Liang, X.; Li, J.; Yang, Y.; Jiang, C.; Guo, Y. Designing salt stress-resilient crops: Current progress and future challenges. *J. Integr. Plant Biol.* **2024**, *66*, 303–329. [CrossRef] [PubMed]
55. Choudhary, S.; Wani, K.; Naeem, M.; Khan, M.; Aftab, T. Cellular responses, osmotic adjustments, and role of osmolytes in providing salt stress resilience in higher plants: Polyamines and nitric oxide crosstalk. *J. Plant Growth Regul.* **2023**, *42*, 539–553. [CrossRef]
56. Ueda, A.; Yamamoto-Yamane, Y.; Takabe, T. Salt stress enhances proline utilization in the apical region of barley roots. *Biochem. Biophys. Res. Commun.* **2007**, *355*, 61–66. [CrossRef]

57. Regni, L.; Del Pino, A.; Mousavi, S.; Palmerini, C.; Baldoni, L.; Mariotti, R.; Mairech, H.; Gardi, T.; D'Amato, R.; Proietti, P. Behavior of four olive cultivars during salt stress. *Front. Plant Sci.* **2019**, *10*, 867. [CrossRef]
58. Yuan, J.; Sun, D.; Lu, Q.; Yang, L.; Wang, H.; Fu, X. Responses of physiology, photosynthesis, and related genes to saline stress in *Cornus hongkongensis* subsp. *tonkinensis* (WP Fang) Q. Y Xiang. *Plants* **2022**, *11*, 940. [CrossRef]
59. Lu, H.; Nkoh, J.; Biswash, M.; Hua, H.; Dong, G.; Li, J.; Xu, R. Effects of surface charge and chemical forms of manganese (II) on rice roots on manganese absorption by different rice varieties. *Ecotoxicol. Environ. Saf.* **2021**, *207*, 111224. [CrossRef] [PubMed]

Disclaimer/Publisher's Note: The statements, opinions and data contained in all publications are solely those of the individual author(s) and contributor(s) and not of MDPI and/or the editor(s). MDPI and/or the editor(s) disclaim responsibility for any injury to people or property resulting from any ideas, methods, instructions or products referred to in the content.